Supplement of Geosci. Model Dev., 12, 3835–3862, 2019
https://doi.org/10.5194/gmd-12-3835-2019-supplement

Geoscientific Model Development
Open Access
EGU

Supplement of

Improved methodologies for Earth system modelling of atmospheric soluble iron and observation comparisons using the Mechanism of Intermediate complexity for Modelling Iron (MIMI v1.0)

Douglas S. Hamilton et al.

Correspondence to: Douglas S. Hamilton (dsh224@cornell.edu)

Table S1. Description of the source regions in Fig. 1.

Acronym	Region	Latitude	Longitude	Notes
ARAB	Arabian Peninsula & surrounding regions	0 to 50ºN	37.5 to 67.5ºE	Southern border includes Horn of Africa to incorporate dust emissions from there that are not found at the same latitude westward (Luo et al., 2008).
ASIA	Asia	10ºS to 30ºN 30 to 50ºN 50 to 90ºN	67.5 to 180ºE 110 to 180ºE 52.5 to 180ºE	Excludes major desert regions.
AUS	Australia and New Zealand	10 to 90ºS	67.5 to 180ºE	Northern limit defined by general model ITCZ location.
CAF	Central Africa	0 to 15ºN	45ºW to 37.5ºE	Northern border separates dust and combustion emission sources.
CEAS	Central Asia	30 to 50ºN	67.5 to 110ºE	Major desert region.
EUR	Europe	30 to 50ºN 50 to 90ºN	45ºW to 37.5ºE 45ºW to 52.5ºE	The border between Europe and Asia is along the Volga River (forested land to the west and shrubland to the east (Loveland et al., 2000)).
NAF	North Africa	15 to 30ºN	45ºW to 37.5ºE	
NAM	North America	0 to 90ºN	45 to 180ºW	The eastern border extends through western Greenland to capture combustion emissions off the east coast of the United States.
SAF	South Africa	0 to 90ºS	30ºW to 67.5ºE	Northern limit defined by general model ITCZ location.
SAM	South America	0 to 90ºS	30 to 180ºW	Northern limit defined by general model ITCZ location.

Table S2. Dust atmospheric lifetime (days) in BAM-Fe (CAM4) and MIMI (CAM5). Global annual total emissions of dust also shown under model name.

	Dust lifetime /days	
	BAM-Fe (1800 Tg /a)	MIMI (3200 Tg /a)
Fine/Accumulation	10	6.5
Coarse	3.8	2.0
Fine/Accumulation + Coarse	3.9	2.1

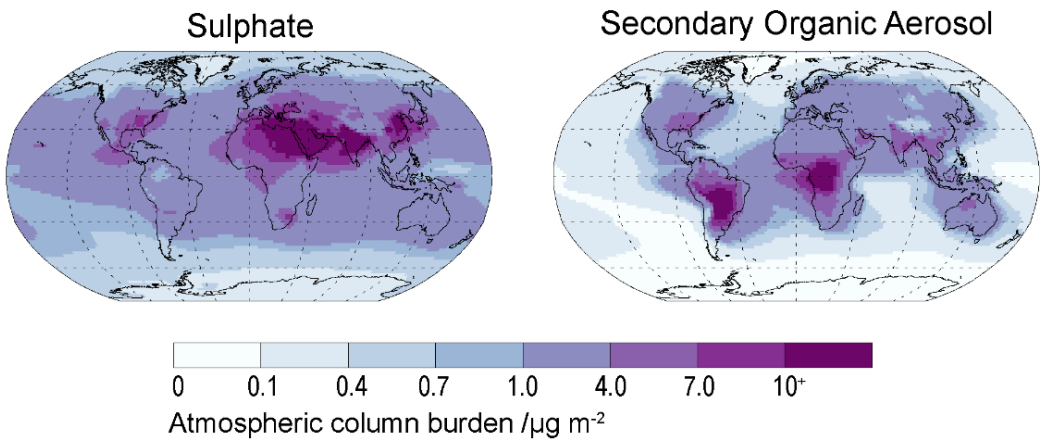

Figure S1. Atmospheric annual mean column burden of sulphate and secondary organic aerosol for year 2007.

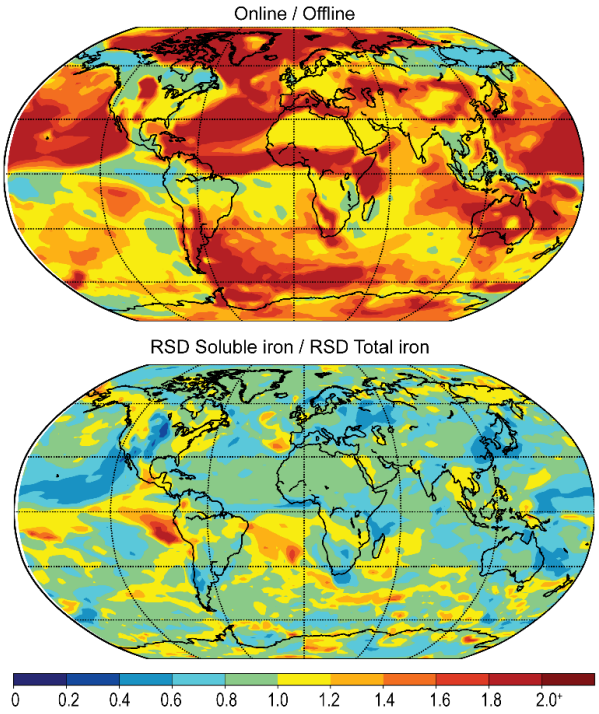

Figure S2. **Top:** Ratio of the online and offline calculation for iron solubility. **Bottom:** Ratio of the relative standard deviation (RSD) of soluble and total iron.

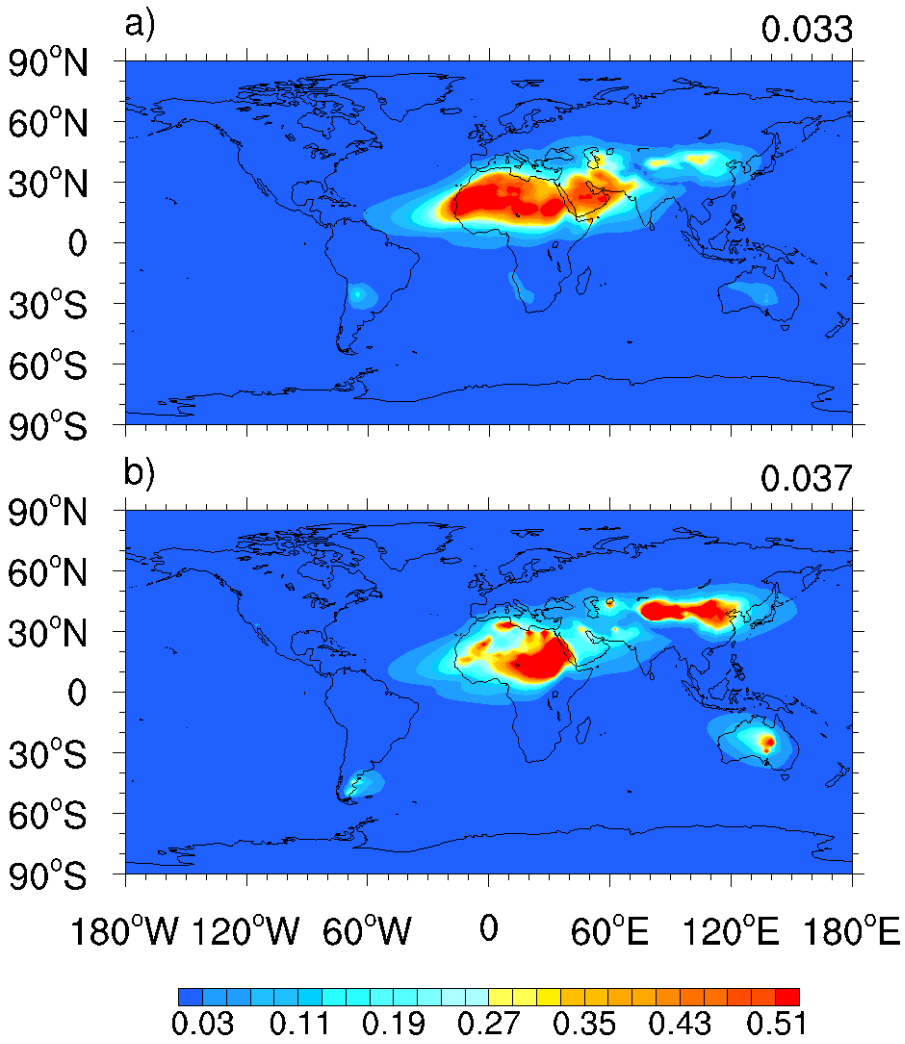

Figure S3. Dust aerosol optical depth within CAM5 MAM4 using: **(a)** the Kok et al. (2014) scheme and **(b)** DEAD (Zender et al., 2003) scheme. Numbers on the top right of each panel represent the globally means.

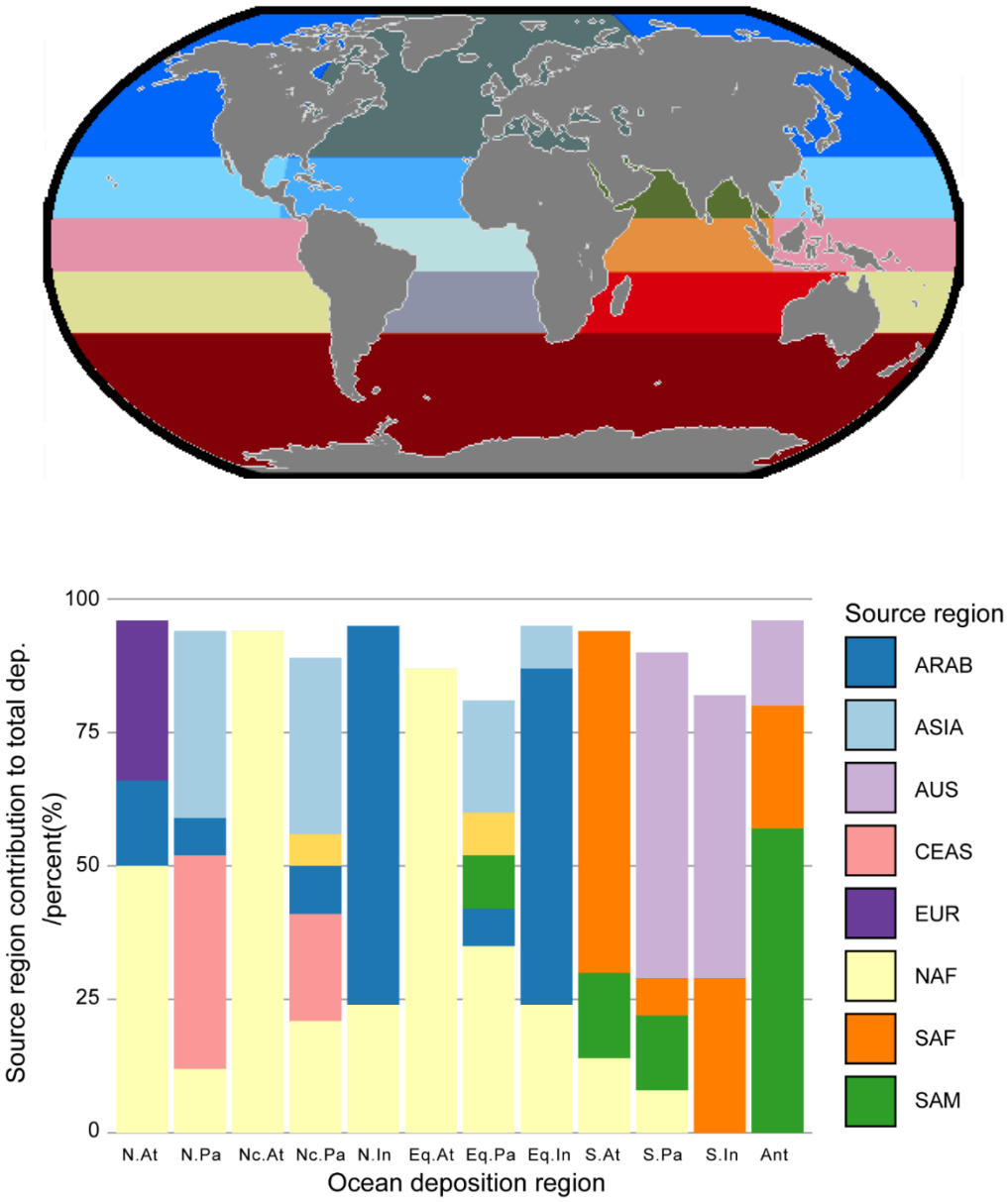

Figure S4. **Top:** Boundary of each ocean regions as defined in Gregg et al. (2003). Note that colours bear no relationship to any other figure. **Bottom:** Contribution of each emission source region (Fig. 1) to the total iron deposition across the region as defined in Gregg et al. (2003). Regions contributing <5% filtered out.

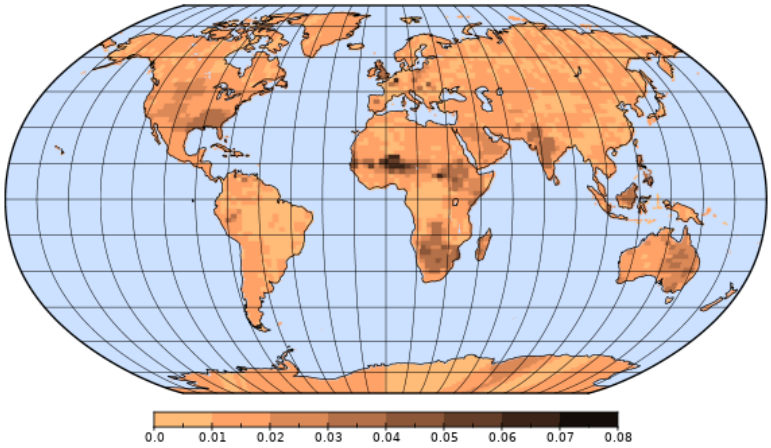

Figure S5. Fraction of the soil mineral which is hematite in MIMI**.**

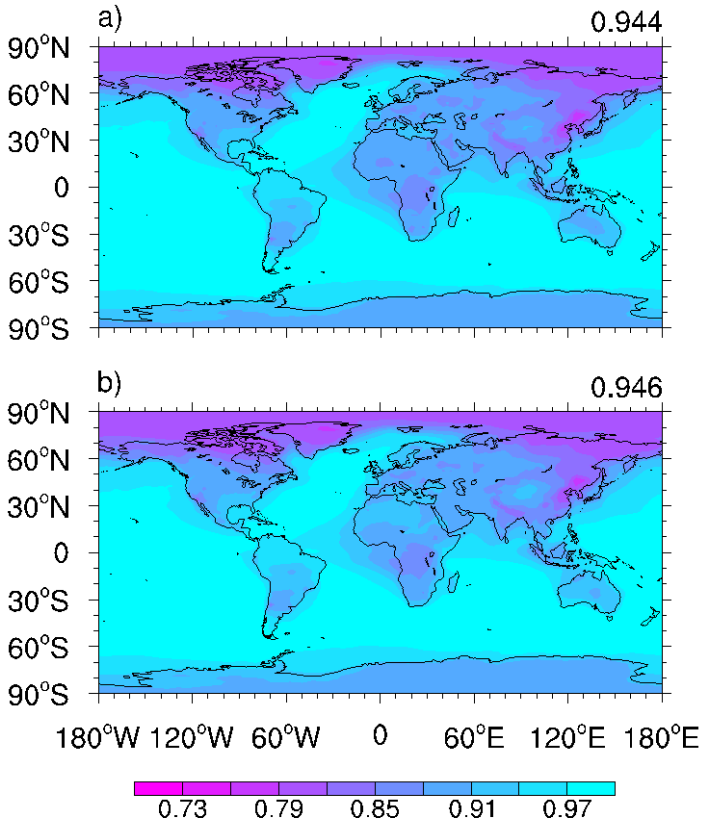

Figure S6. Single scattering albedo with hematite from both clay and silt minerals (a), and solely from clay minerals (b). Number on the top right of each panel represents the global mean value.

References:

Gregg, W. W., Conkright, M. E., Ginoux, P., O'Reilly, J. E. and Casey, N. W.: Ocean primary production and climate: Global decadal changes, Geophys. Res. Lett., 30(15), 10–13, doi:10.1029/2003GL016889, 2003.

Kok, J. F., Mahowald, N. M., Fratini, G., Gillies, J. A., Ishizuka, M., Leys, J. F., Mikami, M., Park, M. S., Park, S. U., Van Pelt, R. S. and Zobeck, T. M.: An improved dust emission model - Part 1: Model description and comparison against measurements, Atmos. Chem. Phys., 14(23), 13023–13041, doi:10.5194/acp-14-13023-2014, 2014.

Loveland, T. R., Reed, B. C., Ohlen, D. O., Brown, J. F., Zhu, Z., Yang, L. and Merchant, J. W.: Development of a global land cover characteristics database and IGBP DISCover from 1 km AVHRR data, Int. J. Remote Sens., 21(6–7), 1303–1330, doi:10.1080/014311600210191, 2000.

Luo, C., Mahowald, N., Bond, T., Chuang, P. Y., Artaxo, P., Siefert, R., Chen, Y. and Schauer, J.: Combustion iron distribution and deposition, Global Biogeochem. Cycles, 22(GB1012), 1–17, doi:10.1029/2007GB002964, 2008.

Zender, C. S., Bian, H. and Newman, D.: Mineral Dust Entrainment and Deposition (DEAD) model: Description and 1990s dust climatology, J. Geophys. Res., 108(D14), doi:10.1029/2002JD002775, 2003.